



Published in final edited form as:

J Immunol. 2023 December 15; 211(12): 1751–1755. doi:10.4049/jimmunol.2200829.

CCR8 Signaling Regulates IL-25- and IL-33-Responsive Skin Group 2 Innate Lymphoid Cell Migration and Function

Zhengwang Sun¹, Sen Han², Xueping Zhu¹, Sabina A. Islam^{1, #}

¹Center for Immunology and Inflammatory Diseases, Massachusetts General Hospital, Harvard Medical School.

²Center for Vaccine Research, Massachusetts General Hospital, Harvard Medical School.

Abstract

Group 2 innate lymphoid cells (ILC2s) are sentinels of barrier immunity, and their activation by the epithelial alarmins IL-25 and IL-33 is a defining trait. Here we identified a role for the chemokine receptor CCR8 in modulating skin ILC2 abundance and activation. CCR8 signaling facilitated IL-25 induced increases in skin and lung ILC2s, ILC2 activation and systemic IL-13 production, and ligand directed ILC2 entry into skin and lung. CCR8 controlled ILC2 tissue entry in IL-25 treated naïve mice, but only transferred bone marrow ILC2 progenitors were equipped to enter the skin whereas multiple tissue sourced ILC2s entered the lung. CCR8 selectively regulated IL-33 induced increases in skin ILC2s, their proliferation, and production of IL-13/IL-5, as well as IL-33-responsive transferred ILC2 trafficking only to the skin. Collectively, we illuminate novel aspects of CCR8 signaling regulated ILC2 motility and function, especially in the skin, in response to two hallmark ILC2 activating alarmins.

INTRODUCTION

GATA-3 dependent group 2 ILCs (ILC2s) produce IL-4, IL-5, IL-9, and IL-13 upon activation by the epithelial alarmins TSLP, IL-33, and IL-25 (1, 2). CCR8 is a signature gene of the mouse ILC2 transcriptome (3). CCR8 induces Th2 cell migration through its ligands CCL1, mCCL8 (mouse) and CCL18 (4-6). CCR8 ligands are highly upregulated in allergic disorders such as asthma and atopic dermatitis(1, 7). The chemokine receptors CCR8 and CCR4 are selectively enriched in ILC2s but have tissue specific differences in expression. Gut ILC2s highly express CCR4, whereas lung and skin ILC2s highly express CCR8 (3, 8). The role of CCR8 in skin ILC2 migration remains to be elucidated.

mCCL8 and CCR8 were shown to be essential for ILC2 motility and activation within the lung after IL-33 challenge (9). In contrast, CCR8 signaling was irrelevant for transferred

[#]Corresponding author Center for Immunology and Inflammatory Diseases, Massachusetts General Hospital, Harvard Medical School. Author contributions (CRediT-compliant)

Z.W. Sun designed and performed experiments, curated and analyzed data, and wrote the manuscript. S. Han helped with tissue harvest and single cells preparation. X. Zhu helped with data analysis. S. A. Islam conceptualized and designed the study, acquired funding for the study, supervised the study, performed experiments, interpreted data, and wrote the manuscript.

Conflict of Interest Statement

The authors declare there is no conflict of interest.

ILC2 migration into papain treated lungs but was important for autocrine/paracrine feed forward signaling through CCL1 in promoting ILC2 expansion and effector function during helminth infection (10). Here we define a unique specificity of the CCR8-axis in promoting IL-25 and IL-33 induced increases in skin ILC2s, as well as skin ILC2 activation and migration.

MATERIALS AND METHODS

Mice

C57BL/6J mice were purchased from Charles River. CD45.1, IL-13^{tm1(YFP/cre)Lky} (YetCre-13) and IL-5^{tm1.1(icre)Lky(RED5)} mice were obtained from the Jackson Laboratory. *Ccr8*^{-/-} mice were obtained from Sergio Lira (Mount Sinai Hospital, NY). *Ccl8*^{-/-} mice were generated from *Ccl8*^{LacZ/+tm1a} mice from KOMP/MMRRC Repository (UC Davis, CA). All protocols were approved by the Massachusetts General Hospital Subcommittee on Research Animal Care. Mice of both genders were used.

Mouse treatment

Mice were intraperitoneally (i.p.) injected with IL-25 (400 ng/day/mouse) for 3 days, or IL-33 (300 ng/day/mouse) for 7 days. For trafficking experiments, CD45.1X CD45.2 or *Ccl8*^{-/-} recipients were half-lethally exposed to CS¹³⁶ (5G). 24 hrs after transfer, recipients were treated with IL-25 or IL-33 as above.

Tissue cell harvest

Ears and lungs were digested with Liberase (0.1 mg/mL), dissociated with GentleMACS (Miltenyi, MA), and filtered with 70 µm strainers. Cleaned and minced small intestines were digested in HBSS containing 5% FCS and 1 mM DTT. Spleens were mashed on 70 µm strainers. Femurs were flushed to collect bone marrow (BM) that was treated with red blood lysis buffer.

Competitive homing *in vivo*

5 million total leukocytes from BM, lung, or small intestine from WT (CD45.1) and *Ccr8*^{-/-} (CD45.2) mice were mixed at a 1:1 ratio and transferred into half-lethally irradiated recipients (CD45.1 X CD45.2, or *Ccl8*^{-/-} mice). For *Ccl8*^{-/-} (CD45.2) recipients, donor leukocytes from WT (CD45.1) and *Ccr8*^{-/-} (CD45.2) mice were stained with CFSE to distinguish extraneous from endogenous cells.

Flow cytometry

Gating strategy is shown in supplemental Fig1A and fluorochrome-conjugated anti-mouse antibodies used are listed in supplemental Table 1. ILC2s were defined as live singlets that were CD45⁺Lin⁻CD90.2⁺ or for sub-gating analysis CD45⁺Lin⁻CD90.2⁺CD127⁺. Lin⁺ cells were defined as CD3⁺CD19⁺B220⁺CD11b⁺CD11c⁺Gr-1⁺FcγR1⁺Ter119⁺NK1.1⁺. Flow cytometry was done on a CytoFLEX LX (Beckman Coulter, NJ).

RNA extraction and qPCR

RNA was extracted from skin and lung in Trizol and purified using the RNeasy Mini kit (Qiagen, Germany). q-PCR was executed on a LightCycler 96 (Roche, Switzerland), and normalized to GAPDH, using primers listed in supplemental Table 1.

Statistical analysis

Statistical analysis was performed using GraphPad Prism 9 with two-way ANOVA or Student's two-tailed t-test.

RESULTS AND DISCUSSION

IL-25 elicited CCR8 regulated increases in ILC2s and ILC2 activation but not proliferation

Systemic IL-25 treatment increased ILC2 frequencies and numbers in several organs, but fewer ILC2s were detected in *Ccr8*^{-/-} ears and lungs (Fig1A-C; supplemental Fig1B-D). IL-25 induced equal ILC2 proliferation, measured by Ki-67 expression, in WT and *Ccr8*^{-/-} tissues (Fig1B; supplemental Fig1E). IL-25 treatment induced increased IL-25R on KLRG1^{hi} ILC2s in the lung, BM and spleen, that was CCR8 regulated only in the spleen (supplemental Fig1H-I). Induction of high KLRG1 expression marks ILC2 activation (11-13). IL-25 induced a modest but significant increase in KLRG1⁺ activated ILC2s in the ear, but a striking increase in KLRG1⁺ lung, BM and spleen ILC2s (Fig1D; supplemental Fig1E-F). *Ccr8*^{-/-} mice had fewer activated KLRG1⁺ ILC2s in the ear, lung and BM.

Only IL-25-responsive BM sourced ILC2s entered the ear in a CCR8 regulated manner

ILC2s detected in the lung after IL-25 treatment of naïve mice originate in the gut, as naïve gut but not lung ILC2s highly express IL-25R in the steady state, enabling gut ILC2 proliferation, lymphatic entry, and subsequent hematogenous inter-organ trafficking to the lung after S1P-dependent egress from the gut, which gut ILC2s do more efficiently than BM ILC2 progenitors (3, 13). Thus, to define the origin of increased skin ILC2s we initially sorted naïve gut sourced lymphocytes from WT (CD45.1) and *Ccr8*^{-/-} (CD45.2) mice and co-transferred them at a 1:1 ratio into naïve WT (CD45.1 x CD45.2) recipients that were treated with IL-25. We detected rare gut sourced ILC2s in the lung and spleen, but none in the ear (supplemental Fig1J).

Thus, to perform *in vivo* trafficking studies of transferred cells not derived by *in vitro* expansion and to determine the tissue source of IL-25 elicited increased skin ILC2s, we utilized a model of homeostatic tissue disruption associated niche depletion (supplemental Fig1K) (14). A 1:1 ratio of lung, gut, and BM sourced WT (CD45.1) and *Ccr8*^{-/-} (CD45.2) lymphocytes were transferred into half-lethally irradiated recipient (CD45.1 X CD45.2) mice that were treated with IL-25. Only BM sourced ILC2s were meaningfully detected in the ear, suggesting that BM ILC2 progenitors were the primary source of IL-25-elicited increased ILC2s observed in the ear (Fig1E).

More WT BM sourced transferred ILC2s were detected in the ear, lung and spleen of IL-25 treated recipients (Fig1E-F; supplemental Fig1L). More transferred *Ccr8*^{-/-} BM derived ILC2s were detected in the BM of recipients, suggesting that CCR8 signaling enabled IL-25

triggered egress of BM ILC2 progenitors into the bloodstream (Fig1F; supplemental Fig1L-M). Collectively, these data indicate that the observed IL-25 treatment elicited increase in skin ILC2s is a consequence of CCR8 signaling that regulates both ILC2 progenitor egress from the BM, and the subsequent migration and CCR8-dependent entry of ILC2s into the ears of treated mice given the lack of a difference in proliferation.

CCR8 controlled multiple tissue sourced ILC2 entry into the lung after IL-25 treatment

In contrast to the the ear, we detected transferred gut, BM and lung sourced ILC2s in the lung and spleen after IL-25 treatment (Fig1F-G; supplemental Fig1L-M). CCR8 signaling regulated gut, BM and lung derived co-transferred ILC2 entry into the lung in these competitive homing studies.

IL-25 induced CCR8 ligands in target tissue and tissue ligand directed ILC2 homing

IL-25 treatment significantly induced expression of both CCR8 ligands, *Ccl11* and *Ccl18*, in the ear and lung (Fig1H). To define if the CCR8 ligand mCCL8 provided a tissue homing cue that enabled IL-25 triggered ILC2 entry into the ear and lung, we co-transferred equal numbers of CFSE stained WT (CD45.1) and *Ccr8*^{-/-}(CD45.2) BM into sub-lethally irradiated *Ccl18*^{-/-} (CD45.2) mice, that were treated with IL-25. We detected CFSE-labelled WT and *Ccr8*^{-/-} ILC2s in the BM and spleen but labeled WT ILC2s were absent in the ear and lung of the same *Ccl18*^{-/-} recipients, implicating a defect in ILC2 entry into the ear and lung in the absence of ligand (Fig1I).

CCR8 signaling globally facilitated IL-13 production by IL-25-responsive ILC2s

ILC2s constitutively express IL-5 but minimal IL-13, and are activated during Th2 inflammation to secrete more IL-13 and IL-5 (15). To examine if CCR8 regulates ILC2 effector function, we crossed *Ccr8*^{-/-} mice with validated IL-13 reporter (YetCre13) and IL-5 reporter (Red5) mice to generate YetCre x *Ccr8*^{-/-} and Red5 x *Ccr8*^{-/-} mice (15). IL-25 induced IL-13 mRNA production by ILC2s, albeit modestly in the skin compared to the other tissues, but this was globally less in the ear, lung, spleen, and BM of *Ccr8*^{-/-} mice, as detected by YFP expression (Fig2A-B; supplemental Fig2A-B). CCR8 also regulated the generation of activated KLRG1⁺IL-13⁺ILC2s globally, and IL-18R⁺IL-13⁺ILC2s in the ear but not other tissues (Fig2C-E). IL-25 induced IL-5 production was not regulated by CCR8 (supplemental Fig2C-E).

CCR8 regulated IL-33 elicited increases in ear ILC2s, and their proliferation and activation

Systemic IL-33 treatment induced increased frequencies and numbers of ILC2s in the ear and lung, and ILC2 proliferation (Fig3A-C). A CCR8 signaling modulated effect was limited to the ears in which fewer ILC2s were detected. The frequency of Ki67⁺ proliferating ILC2s was also lower in *Ccr8*^{-/-} ears, and fewer IL-33R⁺ ILC2s and activated KLRG1⁺ ILC2s were detected in *Ccr8*^{-/-} ears (Fig3B, D-E). *Ccr8*^{-/-} ear ILC2s were unlikely to have an intrinsic defect in IL-33 triggered proliferative capacity as ILC2 proliferation in *Ccr8*^{-/-} lung and BM was not reduced, indicating an effect of the local skin milieu (Fig3B).

CCR8 signaling regulated IL-33 elicited BM ILC2 progenitor homing to the ear

We next co-transferred equal numbers of BM from WT and *Ccr8*^{-/-} mice into half-lethally irradiated recipients that were treated with IL-33. More transferred *Ccr8*^{-/-} ILC2s were found in the BM, indicating their retention in the BM, and fewer *Ccr8*^{-/-} ILC2s were detected only in the ear (Fig3F; supplemental Fig1N). No differential homing was seen in the lungs; highlighting the specificity of this CCR8 regulated BM and skin ILC2 trafficking. We confirmed that IL-33 treatment significantly induced tissue expression of *Ccl8* and *Ccl11* to provide tissue cues for directed migration (Fig3G). IL-33 signaling drives ILC2 progenitor egress from the BM, and migration to lung and skin (14). Collectively, our data imply that CCR8 signaling facilitates IL-33-responsive ILC2 progenitor egress from the BM, and the subsequent entry into the skin.

CCR8 regulated IL-5 and IL-13 production by IL-33 activated skin ILC2s

IL-33 treatment induced lower IL-13 and IL-5 in the ears of *Ccr8*^{-/-} reporter mice (Fig4A-C; supplemental Fig2F-H). More IL-5⁺ ILC2s were seen in the BM of *Ccr8*^{-/-} reporter mice, consistent with a reduced capacity of IL-33 activated *Ccr8*^{-/-} ILC2 progenitors to exit the BM (Fig3F and 4C).

A caveat in interpreting the IL-25 associated trafficking studies is the low numbers of transferred ILC2s detected in the ear and BM. However, our studies convincingly demonstrate that CCR8 signaling regulated IL-25-responsive BM, gut and lung sourced co-transferred ILC2 trafficking into the lungs but not of simultaneously transferred control cells (Fig1F-G; supplemental Fig1J, L-M). It is well established that the source of the IL-25-responsive increased ILC2s seen in the lungs of naïve mice after 3 days of treatment are gut-derived activated IL-25R⁺ ILC2s that migrate into the lung, and not lung resident ILC2s which are predominantly IL-33R⁺, in keeping with known neonatal tissue specific imprinting of ILC2 activating receptors (3, 12, 13). The detection of fewer IL-25-elicited ILC2s (Fig1A-D; supplemental Fig1F) and IL-13⁺ ILC2s (Fig2) in *Ccr8*^{-/-} lungs can only be because of a CCR8-dependent defect in ILC2 migration into the lung after S1P dependent egress from the gut, which is a conclusion supported by our trafficking studies.

Our studies reveal that systemic IL-25 treatment elicits inter-organ ILC2 trafficking of BM egressed progenitors into the skin, and is distinct from IL-25 elicited gut egressed ILC2 inter-organ migration to the lung (12, 13). Skin tropic BM ILC2 progenitors are conditioned to primarily express IL-18R, which marks a population transcriptionally programmed for homing to and function in the skin, some of which co-express IL-25R to allow IL-25-responsiveness (Fig2E; supplemental Fig1H-I)(3). Source tissue heterogeneity may explain discrepancies in CCR8-dependent migration by cultured mouse versus human ILC2 cell lines (9, 10). Though systemic IL-25 and IL-33 treatment elicited increases in lung ILC2 abundance, this was discordantly dependent on CCR8 signaling, which was substantiated by our competitive homing studies. Thus, whether ILC2s engage CCR8 for homing to the lung also depends on the specific inflammatory cue.

Our studies collectively support the conclusion that CCR8 signaling dependent decreased exogenous migration into the ears and lungs was an important primary cause of the

decreased ILC2 abundance seen in *Ccr8*^{-/-} mice after IL-25 treatment. However, *Ccr8*^{-/-} BM ILC2 progenitors revealed less activation, measured by KLRG1 expression, and less IL-13 production after systemic IL-25 treatment, and this was independent of IL-25R or IL-18Ra expression (Fig1D, Fig2A-E; supplemental Fig1H-I, and data not shown). Systemic IL-25 treatment elicits CCL1 production by tissue ILC2s and autocrine CCR8-CCL1 signaling enhances ILC2 activation (10). This likely explains the reduced activation of *Ccr8*^{-/-} BM ILC2 progenitors, which undoubtedly contributed to the decreased abundance of *Ccr8*^{-/-} skin ILC2s after IL-25 treatment.

ILC2s are implicated in homeostatic tissue repair and IL-33 mediated cutaneous wound healing (1, 16). Trauma to the skin, manifested by tape-stripping, produces detectable serum IL-33; tape-stripping elicited serum IL-33 is comparable to serum IL-33 elicited by intranasal fungal challenge, and the latter is sufficient to initiate ILC2 egress from the BM into blood, followed by migration into the lung (14, 17, 18). The reduced frequency of Ki67⁺ proliferating ILC2s in IL-33 treated *Ccr8*^{-/-} ear but not lung or BM ILC2s indicates a local skin-specific effect (Fig 3B). Our data support a model in which skin trauma elicited local IL-33 induces CCR8-mediated resident skin ILC2 activation and expansion that is enhanced by autocrine/paracrine CCL1 signaling, and skin trauma elicited systemic IL-33 elicits CCR8-mediated hematogenous deployment of BM ILC2s (10, 14).

Our data espouses the concept of a tightly regulated BM-skin homing axis that mediates IL-25 and IL-33 triggered exogenous ILC2 entry into the skin that is facilitated by CCR8 signaling. Fate mapping has shown that in contrast to the stable tissue resident lung and gut ILC2 pools that are non-migratory and maintained by self-renewal, the skin and BM ILC2 pools undergo continuous turnover and expansion in the steady state (19). Teleologically, the rapid turnover and continued expansion of ILC2 pools in the BM and skin may signify a centrally controlled BM-skin axis that allows alarmins to rapidly deploy BM progenitors to the skin, given the skin's greater physical vulnerability. Kaede photoconvertible mice have revealed steady state blood borne ILC2 entry into the skin (20). Our data establish that CCR8 signaling partly regulates BM ILC2 progenitor egress and subsequent homing to the skin during IL-25 and IL-33-elicited inflammation.

In summary, our findings support the overall conclusion that CCR8 signaling mediates *in vivo* ILC2 trafficking, and provides clarity to prior studies(9, 10). CCR8 signaling regulated IL-25-induced ILC2 activation, global IL-13 production, and mCCL8-directed migration into the skin and lung. CCR8 was important for IL-33-induced skin ILC2 proliferation, IL-13 and IL-5 production, and ILC2 trafficking to the skin. We found that skin ILC2s robustly produced IL-13 upon TSLP and IL-18 stimulation, independent of CCR8 (supplemental Fig2I-L). We found an additive but not synergistic effect of simultaneous IL-25 and IL-33 treatment in increasing skin ILC2 abundance (supplemental Fig2M). Collectively, we define a unique skin specificity of the CCR8-axis in promoting ILC2 activation and expansion in response to two major barrier alarmins.

Supplementary Material

Refer to Web version on PubMed Central for supplementary material.

Acknowledgments

This work was supported by the National Institutes of Health (R01 AI121248).

References

- Rodriguez-Rodriguez N, Gogoi M, and McKenzie ANJ. 2021. Group 2 Innate Lymphoid Cells: Team Players in Regulating Asthma. *Annu Rev Immunol* 39: 167–198. [PubMed: 33534604]
- Vivier E, Artis D, Colonna M, Diefenbach A, Di Santo JP, Eberl G, Koyasu S, Locksley RM, McKenzie ANJ, Mebius RE, Powrie F, and Spits H. 2018. Innate Lymphoid Cells: 10 Years On. *Cell* 174: 1054–1066. [PubMed: 30142344]
- Ricardo-Gonzalez RR, Van Dyken SJ, Schneider C, Lee J, Nussbaum JC, Liang HE, Vaka D, Eckalbar WL, Molofsky AB, Erle DJ, and Locksley RM. 2018. Tissue signals imprint ILC2 identity with anticipatory function. *Nat Immunol* 19: 1093–1099. [PubMed: 30201992]
- Zingoni A, Soto H, Hedrick JA, Stoppacciaro A, Storlazzi CT, Sinigaglia F, D'Ambrosio D, O'Garra A, Robinson D, Rocchi M, Santoni A, Zlotnik A, and Napolitano M. 1998. The chemokine receptor CCR8 is preferentially expressed in Th2 but not Th1 cells. *J Immunol* 161: 547–551. [PubMed: 9670926]
- Islam SA, Chang DS, Colvin RA, Byrne MH, McCully ML, Moser B, Lira SA, Charo IF, and Luster AD. 2011. Mouse CCL8, a CCR8 agonist, promotes atopic dermatitis by recruiting IL-5+ T(H)2 cells. *Nat Immunol* 12: 167–177. [PubMed: 21217759]
- Islam SA, Ling MF, Leung J, Shreffler WG, and Luster AD. 2013. Identification of human CCR8 as a CCL18 receptor. *J Exp Med* 210: 1889–1898. [PubMed: 23999500]
- Guttman-Yassky E, Bissonnette R, Ungar B, Suarez-Farinas M, Ardeleanu M, Esaki H, Suprun M, Estrada Y, Xu H, Peng X, Silverberg JI, Menter A, Krueger JG, Zhang R, Chaudhry U, Swanson B, Graham NMH, Pirozzi G, Yancopoulos GD, and JD DH. 2019. Dupilumab progressively improves systemic and cutaneous abnormalities in patients with atopic dermatitis. *J Allergy Clin Immunol* 143: 155–172. [PubMed: 30194992]
- Kobayashi T, Voisin B, Kim DY, Kennedy EA, Jo JH, Shih HY, Truong A, Doebel T, Sakamoto K, Cui CY, Schlessinger D, Moro K, Nakae S, Horiuchi K, Zhu J, Leonard WJ, Kong HH, and Nagao K. 2019. Homeostatic Control of Sebaceous Glands by Innate Lymphoid Cells Regulates Commensal Bacteria Equilibrium. *Cell* 176: 982–997 e916. [PubMed: 30712873]
- Puttur F, Denney L, Gregory LG, Vuononvirta J, Oliver R, Entwistle LJ, Walker SA, Headley MB, McGhee EJ, Pease JE, Krummel MF, Carlin LM, and Lloyd CM. 2019. Pulmonary environmental cues drive group 2 innate lymphoid cell dynamics in mice and humans. *Sci Immunol* 4.
- Knipfer L, Schulz-Kuhnt A, Kindermann M, Greif V, Symowski C, Voehringer D, Neurath MF, Atreya I, and Wirtz S. 2019. A CCL1/CCR8-dependent feed-forward mechanism drives ILC2 functions in type 2-mediated inflammation. *J Exp Med* 216: 2763–2777. [PubMed: 31537642]
- Flamar AL, Klose CSN, Moeller JB, Mahlaköiv T, Bessman NJ, Zhang W, Moriyama S, Stokic-Trtica V, Rankin LC, Putzel GG, Rodewald HR, He Z, Chen L, Lira SA, Karsenty G, and Artis D. 2020. Interleukin-33 Induces the Enzyme Tryptophan Hydroxylase 1 to Promote Inflammatory Group 2 Innate Lymphoid Cell-Mediated Immunity. *Immunity* 52: 606–619.e606. [PubMed: 32160524]
- Huang Y, Guo L, Qiu J, Chen X, Hu-Li J, Siebenlist U, Williamson PR, Urban JF Jr., and Paul WE. 2015. IL-25-responsive, lineage-negative KLRG1(hi) cells are multipotential 'inflammatory' type 2 innate lymphoid cells. *Nat Immunol* 16: 161–169. [PubMed: 25531830]
- Huang Y, Mao K, Chen X, Sun MA, Kawabe T, Li W, Usher N, Zhu J, Urban JF Jr., Paul WE, and Germain RN. 2018. S1P-dependent interorgan trafficking of group 2 innate lymphoid cells supports host defense. *Science* 359: 114–119. [PubMed: 29302015]
- Stier MT, Zhang J, Goleniewska K, Cephys JY, Rusznak M, Wu L, Van Kaer L, Zhou B, Newcomb DC, and Peebles RS Jr. 2018. IL-33 promotes the egress of group 2 innate lymphoid cells from the bone marrow. *J Exp Med* 215: 263–281. [PubMed: 29222107]

15. Nussbaum JC, Van Dyken SJ, von Moltke J, Cheng LE, Mohapatra A, Molofsky AB, Thornton EE, Krummel MF, Chawla A, Liang HE, and Locksley RM. 2013. Type 2 innate lymphoid cells control eosinophil homeostasis. *Nature* 502: 245–248. [PubMed: 24037376]
16. Rak GD, Osborne LC, Siracusa MC, Kim BS, Wang K, Bayat A, Artis D, and Volk SW. 2016. IL-33-Dependent Group 2 Innate Lymphoid Cells Promote Cutaneous Wound Healing. *J Invest Dermatol* 136: 487–496. [PubMed: 26802241]
17. Karta MR, Rosenthal PS, Beppu A, Vuong CY, Miller M, Das S, Kurten RC, Doherty TA, and Broide DH. 2018. beta2 integrins rather than beta1 integrins mediate *Alternaria*-induced group 2 innate lymphoid cell trafficking to the lung. *J Allergy Clin Immunol* 141: 329–338 e312. [PubMed: 28366795]
18. Leyva-Castillo JM, Galand C, Kam C, Burton O, Gurish M, Musser MA, Goldsmith JD, Hait E, Nurko S, Brombacher F, Dong C, Finkelman FD, Lee RT, Ziegler S, Chiu I, Austen KF, and Geha RS. 2019. Mechanical Skin Injury Promotes Food Anaphylaxis by Driving Intestinal Mast Cell Expansion. *Immunity* 50: 1262–1275 e1264. [PubMed: 31027995]
19. Schneider C, Lee J, Koga S, Ricardo-Gonzalez RR, Nussbaum JC, Smith LK, Villeda SA, Liang HE, and Locksley RM. 2019. Tissue-Resident Group 2 Innate Lymphoid Cells Differentiate by Layered Ontogeny and In Situ Perinatal Priming. *Immunity* 50: 1425–1438 e1425. [PubMed: 31128962]
20. Dutton EE, Gajdasik DW, Willis C, Fiancette R, Bishop EL, Camelo A, Sleeman MA, Coccia M, Didierlaurent AM, Tomura M, Pilataxi F, Morehouse CA, Carlesso G, and Withers DR. 2019. Peripheral lymph nodes contain migratory and resident innate lymphoid cell populations. *Sci Immunol* 4.

Key points

- CCR8 facilitates IL-25 induced skin and lung ILC2 increase and production of IL-13
- CCR8 regulates IL-33-responsive skin ILC2 increase and production of IL-13/IL-5
- CCR8 controls IL-25 induced ILC2 skin and lung homing, and IL-33 induced skin homing

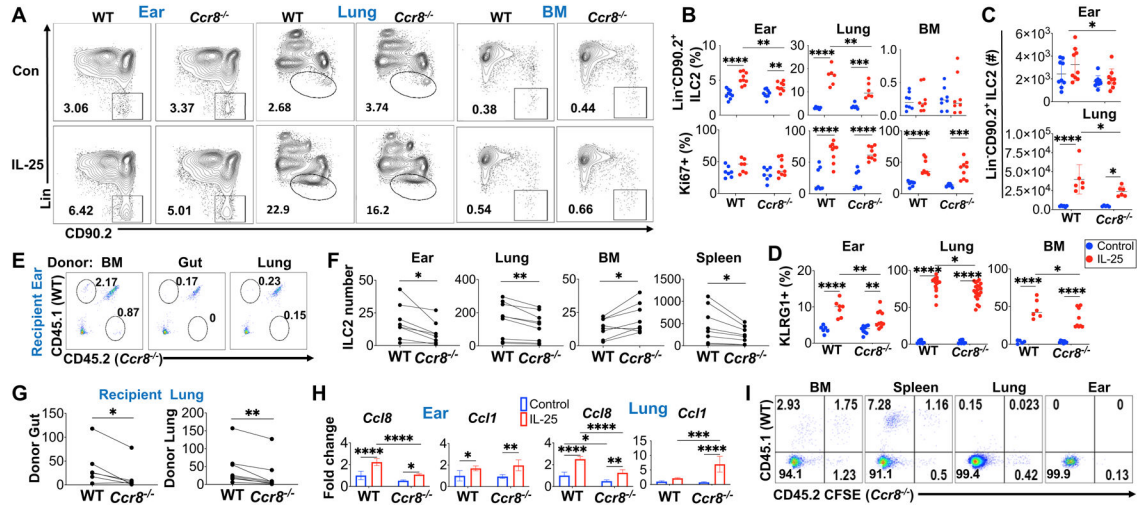


Fig 1. CCR8 promotes IL-25 induced increases in skin and lung ILC2s and ILC2 activation. WT and *Ccr8*^{-/-} (A-D, H), CD45.1xCD45.2 (E-G), and *Ccl8*^{-/-} (I) mice were injected i.p. with IL-25 (400 ng/day/mice) for 3 days and analyzed on day 4. (A) Representative flow plots; and (B) total tissue Lin⁻CD90.2⁺ ILC2 and CD127⁺Ki67⁺ ILC2 percentages after treatment. (C) Counts of skin and lung Lin⁻CD90.2⁺ ILC2s. (D) Percentages of CD127⁺KLRG1⁺ activated ILC2s. (E) Flow plots of co-transferred WT (CD45.1) and *Ccr8*^{-/-} (CD45.2) BM, gut and lung Lin⁻CD90.2⁺ ILC2s in the ears of partially irradiated CD45.1xCD45.2 recipients. (F-G) Tissue accumulation of transferred ILC2s: when sourced from (F) BM; (G) gut and lung. (H) IL-25 induced *Ccl8* and *Ccl1* expression. (I) Flow plots of transferred CFSE-labeled BM sourced WT (CD45.1) and *Ccr8*^{-/-} (CD45.2) ILC2s in irradiated recipient *Ccl8*^{-/-} (CD45.2) mice. Data are representative of three independent experiments except (I) which represents 2 experiments. n=5-14 mice/group with data combined from three independent experiments except (H) which represents 3 biological replicates. Individual data point frequencies represent individual mice, and were calculated per organ: whole lung, both ears, both femurs and spleen per mouse. BM, bone marrow; con, control. Graphs show mean ± SEM; *, *P* < 0.05; **, *P* < 0.01; ***, *P* < 0.001; ****, *P* < 0.0001 by two-way ANOVA (B, C, D, and H) or paired t test (F and G).

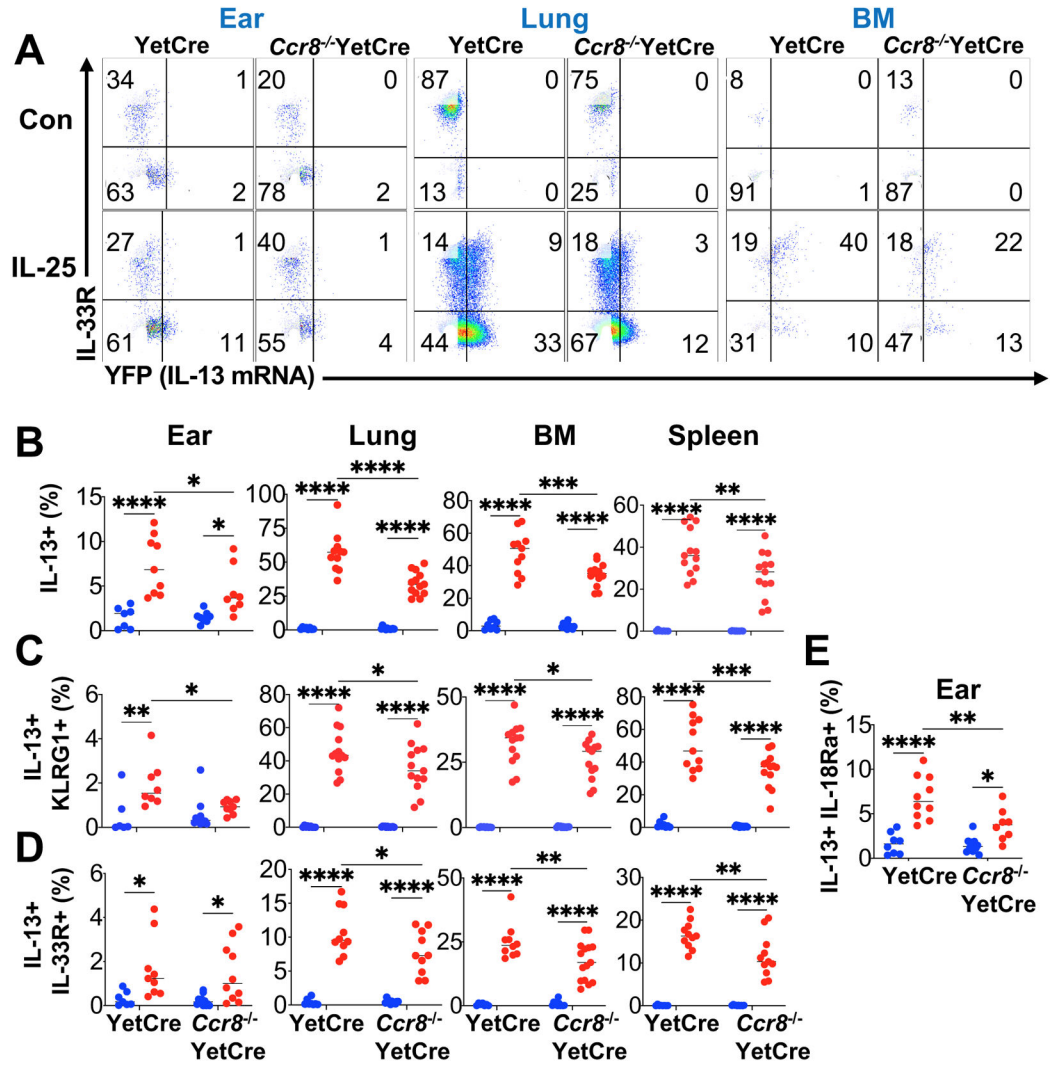


Fig 2. CCR8 facilitates IL-25 induced IL-13 production by ILC2s.

YetCre and *Ccr8*^{-/-} *YetCre* IL-13 reporter mice were injected with IL-25 for 3 days and analyzed on day 4. (A) Representative flow plots of IL-13 production by Lin⁻CD90.2⁺CD127⁺ gated ILC2s. Percentages of (B) total IL-13⁺ ILC2s; and (C-E) IL-13 expressing KLRG1⁺, IL-33R⁺ ILC2s, and IL-18Ra⁺ ILC2s. n=5-13/group with data combined from 3 independent experiments. Graphs show mean ± SEM; *, *P* < 0.05; **, *P* < 0.01; ***, *P* < 0.001; ****, *P* < 0.0001 by two-way ANOVA.

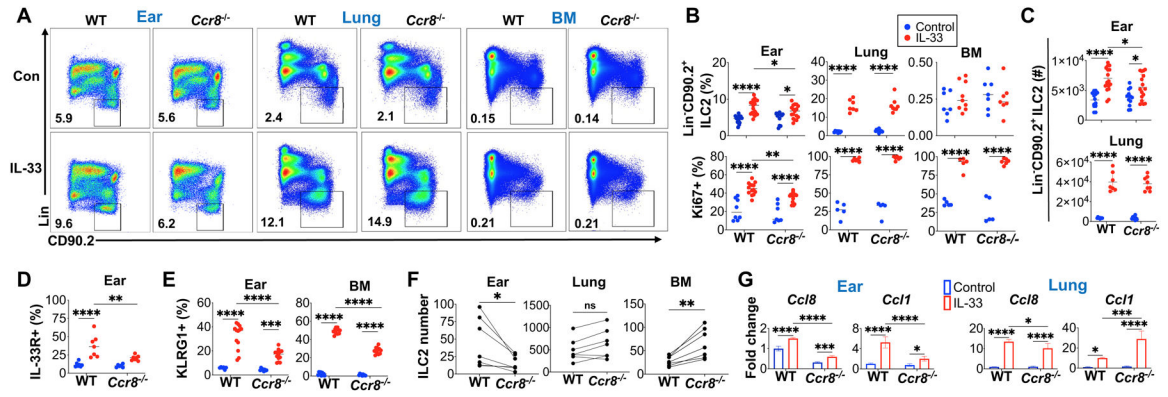


Fig 3. CCR8 aids IL-33 elicited increased skin ILC2s, and their proliferation and activation. WT and *Ccr8*^{-/-} (A-E, G), and CD45.1xCD45.2 (F), mice were injected with IL-33 for 7 days and analyzed on day 8. (A) Representative flow plots of ILC2s. (B) Total tissue Lin⁻CD90.2⁺ ILC2 and CD127⁺Ki67⁺ ILC2 percentages. (C) Counts of skin and lung Lin⁻CD90.2⁺ ILC2s. Percentages of (D) CD127⁺IL-33R⁺; and (E) CD127⁺KLRG1⁺ activated ILC2s. (F) Tissue distribution of BM sourced ILC2s from WT (CD45.1) and *Ccr8*^{-/-} (CD45.2) mice in treated irradiated CD45.1xCD45.2 recipients. (G) IL-33 induced *Ccl8* and *Ccl1* expression. n=5-19 mice/group with data combined from three independent experiments except (G) which represents 3 biological replicates. Graphs show mean ± SEM; *, *P* < 0.05; **, *P* < 0.01; ***, *P* < 0.001; ****, *P* < 0.0001 by two-way ANOVA (B-E, and G) or paired t test (F).

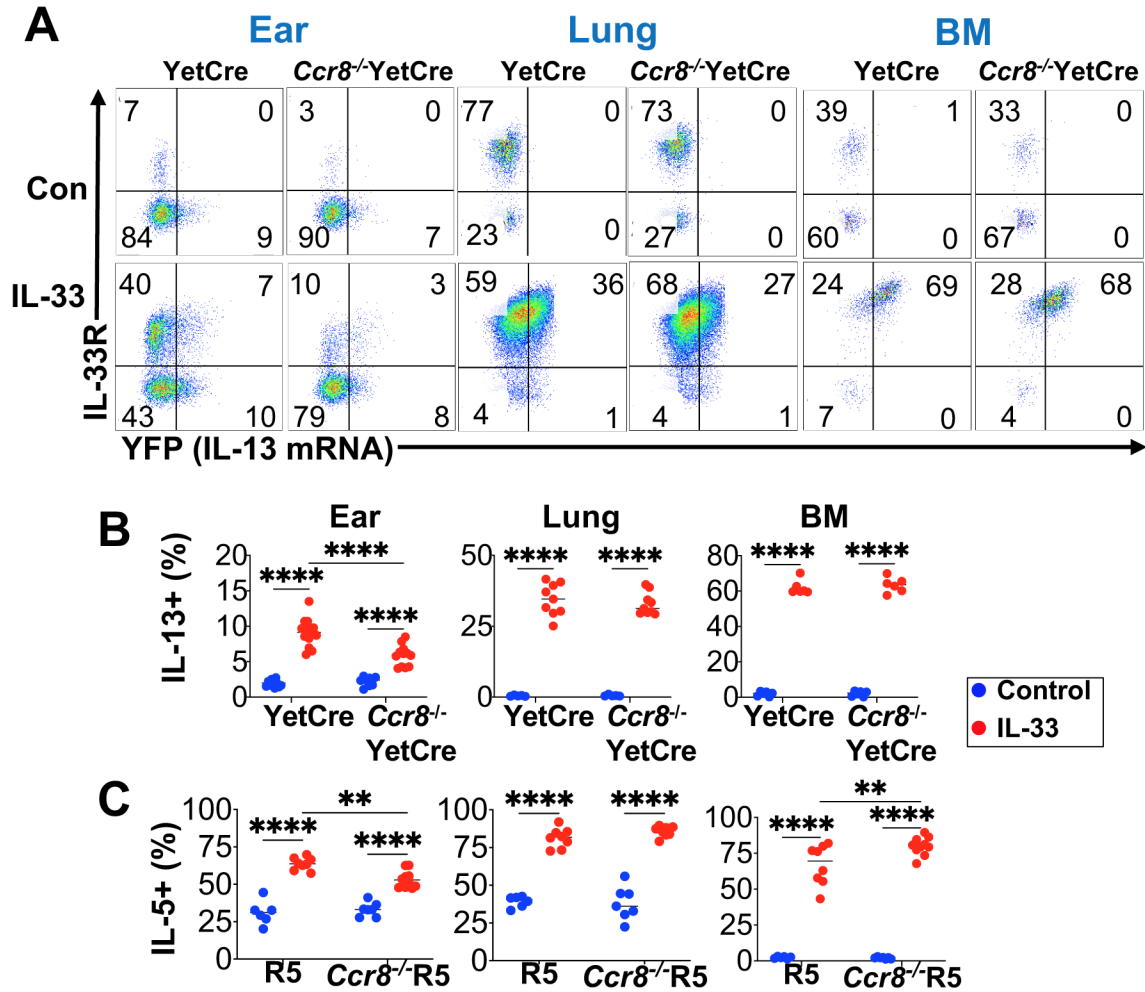


Fig 4. CCR8 promotes IL-13 and IL-5 production by IL-33 activated skin ILC2s. (A-B) *YetCre* and *Ccr8*^{-/-}*YetCre* IL-13 reporter mice and (C) *Red5* and *Red5* x *Ccr8*^{-/-} IL-5 reporter mice were injected with IL-33 for 7 days and analyzed on day 8. (A) Representative flow plots of IL-13 production by Lin⁻CD90.2⁺CD127⁺ gated ILC2s. Percentages of total (B) IL-13⁺ and (C) IL-5⁺ ILC2s. n=5-12/group with data combined from 3 independent experiments. Graphs show mean ± SEM; **, *P* < 0.01; ****, *P* < 0.0001 by two-way ANOVA.